SPE 163867

Fluid Selection for Energized Fracture Treatments

Lionel H. Ribeiro and Mukul M. Sharma, SPE, The University of Texas at Austin

This paper was prepared for presentation at the SPE Hydraulic Fracturing Technology Conference held in The Woodlands, Texas, USA, 4–6 February 2013.

Abstract

As the development of unconventional (e.g., tight gas, shales, coalbed methane) and under-pressured reservoirs has increased, so has the demand for innovative hydraulic fracture designs. The use of gases and foams has experienced a significant resurgence in popularity with the development of unconventional reservoirs and with the growing limitations on water supply in some areas. Until recently, the tools available for fracture design were not capable of modeling hydraulic fracturing with compressible fluids and non-isothermal treatments. Ribeiro and Sharma (2012b) presented a model that was capable of simulating hydraulic fracturing treatments with multi-phase, compressible fracturing fluids with changing temperature, phase behavior, and multi-phase leak-off during the treatment. The main objective of this paper is to show how such a model can be used for screening fracturing fluid candidates and for optimizing energized fracture treatments.

In conducting this study, we have combined this 3-D compositional fracturing model with a multi-phase well-productivity model for hydraulically fractured wells. This paper presents results for slick water, linear gel, gelled CO_2, gelled LPG, N_2 foams and CO_2 foams in a low permeability reservoir. The simulations showed that good proppant placement and high fracture conductivities can be achieved with foams and gelled fluid formulations. LPG, CO_2, and high-quality foams prevent water invasion so they do not impede gas recovery because of water blocking or gel induced damage. In addition, several reservoir parameters appear to control well productivity and therefore fluid selection: (1) relative permeability curves, (2) initial gas saturation, (3) reservoir pressure, and (4) sensitivity to water. The benefits and disadvantages that must be considered when selecting a fracturing fluid are highlighted in this paper and a methodology is proposed to quantify these pros and cons.

Introduction

Various alternatives to water-based fracturing fluids have been developed and successfully implemented in the field over the past forty years. These alternatives include surfactant fluids, energized fluids, emulsions, and non-aqueous fluids. Many fluid formulations exist and the reader may refer to the summary compiled by Gupta (2011) for a more exhaustive list of fracturing fluid candidates. In this paper, energized fluids are defined as fluids containing at least one compressible (“gas-like”) phase. Water-based fluids refer to both slick water and water-based polymer fluids (linear gels and cross-linked gels).

Typically, water-based fluids are the simplest and most cost-effective solution to fracture a rock formation. However, alternatives to water-based fluids have significantly outperformed water treatments in many reservoirs. For instance, foams have been extensively used in the seventies in various depleted reservoirs in which water fractures were not effective. More recently, the development of many unconventional reservoirs (tight gas, shale gas, coalbed methane) has prompted the industry to reconsider “waterless” fracturing treatments as viable alternatives to water-based fracturing fluids. In these reservoirs, the interactions between the rock formation and the fracturing fluids may be detrimental to hydrocarbon production. Numerous authors have shown the benefits of using energized fluids, and the reader may refer to the work of King (1985), Mazza (2001), Tudor *et al.* (2009), Burke *et al.* (2011) and Gupta (2011) for more details.

Why so Many Fracturing Fluids?

The first question one may ask is: why do we have so many different kinds of fracturing fluids? The main motivation behind having a wide range of fracturing fluids is to cope with different rock formations, reservoir fluids, pumping schedules and horsepower requirements. There are several reasons to consider fluids that contain little or no water:

1. Water sensitivity of the formation: The base lithology – i.e. the mineral composition - of a given rock formation impacts the recovery process of water, gas, and oil. For example, oil-based fluids, LPG, CO_2, and high-quality foams are recommended in water-sensitive formations to prevent excessive fines migration and clay swelling. In many shales and clay-rich sands, proppant conductivity drops considerably in the presence of water because the rock-fluid interactions soften the rock leading to proppant embedment
2. Water blocking: In under-saturated gas formations, the invasion (imbibition) of water from the fracturing fluid can be very detrimental to gas productivity as any additional water remains trapped because of capillary retention. The increase in water saturation significantly reduces the relative permeability to gas, sometimes by orders of magnitude (Parekh *et al.* 2004; Mahadevan *et al.* 2005). This adverse phenomenon is referred to as water blocking (or water trapping). The invasion of water in oil-rich reservoirs is not as detrimental because oil is more efficient than gas at displacing water.
3. Proppant placement: Foams and other gelled non-aqueous fluids can transport proppant much more effectively than slick water fluids. At high foam qualities (gas volume fraction typically higher than 0.5), the interactions between gas bubbles cause a large energy dissipation that results in a high effective viscosity (Reidenbach *et al.* 1986; Harris *et al.* 1991 ; Economides and Nolte 2000). At low foam qualities (less than 0.5), the interactions between bubbles are minimal so the fluid viscosity resembles that of the base fluid (which is typically gelled). CO_2 and LPG can also be gelled and the subsequent viscosity is comparable to the viscosity of their gelled water counterpart.
4. Water availability and cost: Operators are limited by the equipment and the fluids readily available on site. As regions such as West Texas remains prone to drought, fresh water can become difficult to obtain. In some areas, the local legislation even limits water usage, which has prompted many operators to use waterless fracturing treatments. Alternatively, the supply and the cost of LPG, CO_2, and N_2 are strongly site-specific. Much of the cost savings depend on the availability of the fluid and the structure of the pumping contractor's bid package. The use of large quantities of gases requires the deployment of many trucks, pressurized storage units, and specific pumping equipment.

It should be noted that all of the above considerations are geared towards achieving the maximum productivity from the well at a low economic and environmental cost. It is shown in this paper that in lieu of a field trial-and-error approach, the use of a good fracturing / well productivity model together with field performance data to predict the performance of different types of fracturing fluids can prove to be a very helpful way to select from a very wide range of fracturing fluids.

Objective and Proposed Methodology

The main objective of this paper is to propose a methodology to answer the following question: which fracturing fluid should I use for a given reservoir? To do so, we follow a modeling approach using a design tool particularly suitable for designing and optimizing energized fracture treatments. Clearly, this modeling approach does not replace field trials. Rather, the modeling approach complements the costly trial-and-error approach. Once the best fluid candidates have been identified with the modeling tool, these fluid formulations can by implemented in the field.

The best fluid candidates are fluids yielding the highest hydrocarbon production and/or the highest rate of return. From a design standpoint, it means that we want to predict the final fracture geometry, the final proppant distribution, the fracture conductivity, and the connection between the initially undamaged reservoir and the fracture. To do so, we have used the compositional 3-D model introduced by Ribeiro and Sharma (2012b) and the PI model presented by Friehauf, Suri, and Sharma (2010). This PI model was combined with the 3-D compositional fracturing model, making the subsequent tool particularly suitable for designing and optimizing energized fracture treatments. This new model does not replace conventional fracturing simulators, which offer many additional features. Rather, it constitutes another tool available to the fracturing engineer to rapidly screen fracturing fluids and to design energized treatments. The fracturing treatment design may then be improved with a commercial simulator if non-energized fluids are thought to perform as well as or better than energized fluids.

In this paper, we present results for six different fluid formulations: slick water, linear gel, supercritical CO_2, LPG, N_2 foams, and CO_2 foams. This list is not intended to be exhaustive. In fact, the effect of any fluid formulation may be investigated as long as we know (1) the fluid rheology, (2) the phase behavior, (3) the leak-off coefficient of each phase, and (4) how the fluid impacts the relative permeability to gas (oil) in the reservoir.

Fracturing Fluid Properties

Phase Density

The fracturing fluid density primarily affects fracture geometry, pump horsepower requirements, and proppant transport. Energized fluids are compressible, so they tend to expand as the rock formation heats up the fracturing fluid. Significant fluid expansion increases the fracture volume. This effect is not captured by traditional isothermal fracturing simulators, which assume that the fracturing fluid remains incompressible. Also, the density of compressible fluids significantly changes as the temperature and the pressure vary from the surface to the downhole conditions. The densities of the many fluid formulations encountered in this paper are well-documented, and we chose to follow the work of Friehauf (2009) to determine phase density as a function of pressure, temperature, and composition.

Fluid Composition

Nitrogen is practically insoluble in water and water does not partition inside the gas phase. For N_2 foams, the liquid phase only contains water and the gas phase only contains nitrogen. CO_2 is appreciably more soluble in water. For CO_2 foams, the liquid phase contains water and some soluble CO_2, and the gas phase only contains CO_2.

Since the gas and the liquid phases leak off at different rates (Harris 1985; Harris 1987; Ribeiro and Sharma 2012a), we want to know how much of each component is invading the rock formation and how much remains inside the fracture. Changes in fluid composition inside the fracture alter the fluid saturations and, therefore, the fluid rheology. The composition of the fluid leaking off alters the water and hydrocarbon saturations inside the rock matrix, which subsequently alters the relative permeability to gas (oil) and, therefore, the gas (oil) production. Changes in fluid pressure during flowback can also alter the fluid saturations substantially. For example, as the bottom hole pressure is decreased during flowback, the CO_2 comes out of solution from the water phase, increasing the gas saturation. This can significantly facilitate the flow of the hydrocarbon fluids to the wellbore. These phase behavior and fluid composition effects are all accurately captured in our fracturing and flowback models.

Rheology

The rheology of linear gels is well-documented. However, rheological data for gelled CO_2 and LPG formulations are very scarce in the literature, and we used the data compiled by Ribeiro (2013). For foams, the fluid rheology is also a function of foam texture. If the foam loses its integrity and breaks, the mixture behaves as two independent phases having different rheology. For unstable foams, gravity segregation quickly splits the two phases, as shown later in this paper.

For stable foams, the two phases travel at the same velocity and there is no slippage. Consequently, the same power-law parameters are assigned to both phases. From a transport standpoint, stable foam is seen as a single "pseudo-phase". The reader may refer to the work of Reidenbach *et al.* (1986), Valko and Economides (1997), and Khade and Shah (2004) for more details on foam rheology. The addition of proppant further complicates the slurry rheology, and the reader may refer to Ribeiro (2013) for empirical correlations describing the rheology of proppant-laden foams.

Impact on Fracture Productivity

Fracture productivity depends on (1) the size of the invaded zone, (2) the relative permeability to gas (oil) in the invaded zone, (3) the filter-cake damage, and (4) the extent of proppant embedment. Most commercial fracturing simulators do not account for all of the adverse mechanisms mentioned above, particularly when foams are used, because these simulators do not distinguish the amount of gas and the amount of liquid leaking off into the rock formation.

The size of the invaded zone is directly related to the amount of fluid leaking off. This is one of the reasons why foams have been successful in under-saturated formations, as foams exhibit lower fluid leak-off (Harris 1985; Harris 1987; Ribeiro and Sharma 2012a). The relative permeability to gas is a direct function of the fluid saturation in the invaded zone. In some reservoirs, water blocking considerably impedes the flow of gas. CO_2, N_2, and LPG preferably mix with the gas phase rather than the water phase. Since the water saturation does not increase, the relative permeability to gas is not affected. For foams, the amount of water invading the rock formation is calculated to estimate water blocking.

The rock formation reacts both chemically and mechanically with the fluid injected. Clays may swell when placed in contact with water, but clays do not interact significantly with CO_2, N_2, and LPG. Furthermore, many unconventional rock formations lose some of their mechanical integrity when placed in contact with water. As the rock becomes softer, the rock further closes on the proppant, thereby promoting proppant embedment.

Modeling

In conducting this study, we have used the compositional 3-D model introduced by Ribeiro and Sharma (2012b) and the PI model presented by Friehauf, Suri, and Sharma (2010). The compositional 3-D hydraulic fracturing model uses compositional and energy balances and couples them with phase behavior; making this model applicable to energized fluids.

The treatment of the fracture mechanics allows for 3-D planar fracture propagation. For each of the simulations presented in this paper, the computation time did not exceed 10 min, which makes the model an efficient screening tool.

Furthermore, the productivity index ratio values are calculated using the PI model presented by Friehauf, Suri, and Sharma (2010). The PI model takes into account varying fracture conductivity and the damage around the fracture face caused by fluid invasion. This model computes the productivity of a fractured well with a finite conductivity fracture and with damage in the invaded zone around and around the wellbore. The reader may refer to Ribeiro and Sharma (2012b) and Ribeiro (2013) for more details about the 3-D fracturing model, and to Friehauf (2009) and Friehauf, Suri, and Sharma (2010) for more details about the productivity calculations. The last two references also constitute the foundations of the 3-D compositional fracturing model.

Example of Fluid Selection

Reservoir Properties and Pumping Schedule

The reservoir chosen for this example is a low-permeability sand formation. The gas-bearing zone is 100 feet in height and is bounded by two shale layers. The fracture gradient is equal to 0.6 psi/ft in the pay zone and to 0.7 psi/ft in the bounding layers. A stress contrast of 120 psi is assumed to be present between the sand and shale layers. **Fig. 1** shows the vertical stress distribution across the three layers and the Young's modulus and Poisson's ratio of each layer. The target zone is perforated along a 50-feet interval. The basic reservoir properties are given in **Table 1**. A typical value of the wall-building leak-off coefficient for this tight gas reservoir is 0.0005 ft/√min in the pay zone and 10^{-6} ft/√min in the bounding layers for the linear gel formulation. The leak-off coefficients for the other fluid formulations are scaled accordingly.

The pumping schedule indicated in **Table 2** is the same for all of the fluid formulations except slick water. The initial pad is followed by two stages of proppant (3 and 6 lbm per added gallon, respectively). In the slick water case, the proppant loading was maintained at 3 lbm per added gallon for both stages to avoid premature screenout. The injection temperature is assumed to be 110°F at the perforations. Seven fluid formulations are considered: slick water, linear gel, supercritical CO_2, LPG, 0.3-quality CO_2 foams, 0.7-quality CO_2 foams, and 0.7-quality N_2 foams. The corresponding fluid properties are given in **Table 3**. These properties are given at a temperature of 110°F and a pressure of 5000 psi simply for reference; they are actually evaluated as a function of pressure and temperature in the model. For the three foam cases, Table 3 provides the foam properties at the foam quality of interest. In particular, the liquid and the gas leak-off coefficients are provided.

Fracture Propagation Results

For the sake of brevity, this paper does not contain all of the relevant outputs (fluid width, proppant distribution, fluid temperature, etc.) obtained with the 3-D compositional simulator for each fluid case. Rather, we chose to present detailed results for the 0.7-quality CO_2 foam, and the most critical results for the other fluid formulations are given in **Table 4**. The choice is motivated by the fact that this is, to our knowledge, the first published example of a simulation of a 3-D fracture initiated with a two-phase mixture using a compositional hydraulic fracturing simulator.

Figs. 2 to 7 present results for the 0.7-quality CO_2 foam treatment. Fig. 2 shows the evolution of total fracture length and height over the 50 minutes of pumping. Figs. 3 to 7 show the fluid fracture width, fluid temperature, CO_2 gas phase density, proppant volumetric concentration, and propped fracture width, respectively, at the end of pumping. The combination of these plots forms a good diagnostic tool to tailor the fracturing treatment.

Fig. 3 shows that the fracture penetrates the upper layer toward the end of pumping. The fracture grows upward as the stress difference between the rock (0.6 psi/ft) and the fluid (0.39 psi/ft) decreases. The stress contrast is relatively small at the interface so the fracture can overcome the stress contrast and penetrates the upper layer. Height containment remains nonetheless satisfactory and the fracture is very thick and rather short. This result is explained by the high-viscosity of the stable foam and by the high rock toughness.

Fig. 4 shows how the fluid temperature rises in the fracture from 110°F at the perforations to 180°F along the fracture tip. Subsequently, Fig. 5 shows how the gas phase expands as the temperature increases. Even though proppant settling is clearly visible in Figs. 6 and 7, the foam was effective at carrying the proppant as far as possible inside the fracture. In fact, most of the fracture located inside the targeted zone is propped. The propped fracture shown in Fig. 7 is then used in the productivity calculations. At the bottom of the fracture, the volumetric proppant concentration reaches the maximum value corresponding to the maximum packing of spheres of equal diameter (0.52).

Remark on Foam Stability

As mentioned previously, we assumed that foam remained stable over time. Therefore, there is no slippage between the two fluid foam phases, and interfacial forces prevent gravity segregation. This assumption is critical as evidenced by **Figs. 8 and 9**. Fig. 8 shows the water saturation inside the fracture after pumping stable 0.7-quality CO_2 foam for 5 minutes. In this case, the water saturation slowly decreases from 0.3 at the perforations to 0.25 along the fracture tip. The fracture is slightly

enriched in the gas phase because the liquid leak-off is higher than the gas leak-off. Alternatively, Fig. 9 shows the water saturation inside the fracture after pumping unstable 0.7-quality CO_2 foam for 5 minutes. Unstable foam refers here to a mixture in which the interfacial forces are not capable of holding the gas bubbles inside the external liquid phase. As the gas bubbles coalescence, the gas pocket migrates upward because of gravity segregation. After only 5 min of pumping, the water and the gas phases are completely separated and the mixture loses its viscosity.

Fracture Productivity Results

For a given reservoir and pumping schedule, the main inputs of the well productivity (PI) model consist of (1) the propped fracture geometry, (2) the mass of each component leaking off into the rock formation, and (3) the conductivity of the propped fracture. The main output of the PI model is the productivity index, which is the fracture productivity (J) of a given treatment normalized by a base productivity. In this paper, the base productivity is the productivity of an unfractured, undamaged, well in a circular drainage area (J_0).

Table 4 and **Fig 10** show the critical dimensionless parameters describing fracture performance. We assumed here that the well was immediately flowed back at the end of pumping. The dimensionless fracture productivity is closely related to three significant parameters used by Friehauf, Suri, and Sharma (2010): dimensionless propped length (L_f/L_{re}), dimensionless fracture conductivity (F_{cd}), and dimensionless permeability in the invaded zone (k_d/k). These numbers form a useful diagnostic tool to identify why a fracturing treatment may underperform. They can be used to tailor "engineered" fracturing treatments. Using the results shown in Table 4, we can draw the following conclusions for this given example:

1. For all of the fluid formulations, the fractures are too short (as evidenced by the values of L_f/L_{re}). If the total amount of fluid pumped over 50 min is reasonable, it would be beneficial to pump a larger pad volume or to pump the subsequent stage at a faster rate to limit the impact of fluid leak-off toward the end of pumping.
2. The proppant was effectively transported by most fluids (except slick water) and the fracture conductivities are satisfactory. The main reasons are that the gelled formulations are quite viscous, and the fractures are fairly short (so it is easier to push the proppant toward the tip).
3. The damage associated with the formation of the gelled filter-cake is not explicitly accounted for in this study. Also, the conductivity of the proppant pack is not an explicit function of the applied stress. Rather, the conductivity of the proppant pack is an input that is proper to each fluid formulation and stress regime. This critical input is often overlooked even though it plays a critical role (Vincent 2002).
4. As anticipated, the damage in the invaded zone is strongly dependent on the nature of the fluid. Water invasion causes a large drop in the relative permeability to gas. This being said, only very large drops in the gas permeability significantly affect the gas production. The damage is noticeable when the dimensionless permeability decreases by two orders of magnitudes.
5. LPG, CO_2, and high-quality foams did not impede gas recovery, as evidenced by the high-values of k_d/k.
6. For this given reservoir and this given pumping schedule, the high-quality foams and pure CO_2 seem to outperform the other fluid formulations. CO_2 outperforms LPG because CO_2 is denser, which in this specific example limits vertical growth.

Reservoir Sensitivity Results

Impact of Fluid Retention on the Relative Permeability to Gas

It is evident from the results presented thus far that the reduction in the gas (oil) relative permeability - both in the rock matrix and in the fracture – largely affects well productivity. The impact of water on the relative permeability to gas depends very much on the initial water saturation in the reservoir and on the end point gas permeability; both of which depend on the single phase permeability of the rock. **Fig. 11** shows three examples of relative permeability curves. Reservoir #1 refers to an under-saturated rock with low initial water saturation, which is typical of a dry gas reservoir (S_{gr}=0.25, S_{wr}=0.1, n_g=2.7, and $k_{rg,0}$=0.8). Reservoir #2 refers to a rock with fairly typical initial water saturation (S_{gr}=0.25, S_{wr}=0.3, n_g=2.5, and $k_{rg,0}$=0.5). Reservoir #3 is a strongly water-wet reservoir with high initial water saturation (S_{gr}=0.1, S_{wr}=0.5, n_g=2, and $k_{rg,0}$=0.2). For these three cases, a small change in gas saturation can change the relative permeability to gas by up to two orders of magnitude (from 0.001 to 0.1). This sharp transition occurs at the transition from immobile to mobile gas, near the residual gas saturation. Then, a very large change in gas saturation is necessary to increase the relative permeability to gas from 0.1 to its maximum value.

The impact of water invasion in these three reservoirs can be very different as shown in **Fig. 12**. Fig. 12 shows the productivity index (J/J_0) dependence on the effective permeability in the invaded zone (k_d/k) and on the depth of penetration of the invaded zone (for cases of 1 inch, 1 foot, and 10 feet, respectively). The size of the invaded zone is mainly dependent

on the amount of fluid leak-off. The amount of permeability damage (k_d/k) is dependent on the capillary properties of the formation and the drawdown pressure (which is the difference between the reservoir pressure and the flowing bottom hole pressure) across the invaded zone. This ratio is equal to the relative permeability to gas (as given by Fig. 11) if the rock formation does not appreciably react – both chemically and mechanically - with water. In this case, the petrophysics of the formation is modeled by simple relative permeability and capillary pressure models, and the damage is created by the presence of high water saturation. However, some rocks that contain clays and other fines are sensitive to water. In this case, clay swelling, fines migration, and chemical reactions can further reduce the value of k_d/k. This ratio can therefore be used as a modeling parameter useful to account for water sensitivity effects in the invaded zone.

For cases with moderate leak-off, the reduction in well productivity is negligible if the ratio k_d/k is higher than 0.1. This is because the reduction in permeability only occurs across a small layer around the fracture. As the ratio k_d/k goes from 0.001 to 0.1, the productivity index increases by a factor of three. As mentioned previously, the ratio k_d/k is very sensitive to the gas saturation. Therefore, a small change in gas saturation (associated with fluid leak-off) can dramatically change the effective permeability in the invaded zone, which results in a significant change in well productivity. For cases with large fluid leak-off, the change in well productivity is more gradual and permeability damage becomes significant at a higher range (as k_d/k goes from 0.005 to 0.2).

Critical Reservoir Properties from a Design Standpoint

Together, Figs. 11 and 12 constitute a simple diagnostic tool to identify when energized fluids are likely to outperform water-based fracturing fluids. The analysis of Figs. 11 and 12 shows that it is critical to maintain a gas saturation slightly higher than the residual gas saturation to yield satisfactory gas flow. The transition between immobile and mobile gas is very steep, as shown in Fig 11. If the gas saturation becomes close to the residual gas saturation after water invasion, energized fluids should be used. When foams are used, knowing the amount of gas (which may be soluble gas) leaking into the rock formation is critical to evaluate the impact on gas saturation, and therefore on well productivity. As long as there is *enough* gas in and around the fracture, well productivity is satisfactory. A criteria to quantify what is meant by *enough* is to identify the foam quality that gives a saturation high enough that k_d/k is higher than 0.1.

Similarly, many more sensitivity plots may be generated to identify critical reservoir parameters. These parameters include relative permeability curves, initial gas saturation, reservoir pressure, and sensitivity to water:

1. Relative permeability curves: The residual gas and water saturations determine the range of allowed gas saturations and control the fractional flow of gas and water. The endpoint relative permeability to gas controls the maximum rate of gas delivery.
2. Initial gas saturation: In under-saturated rocks, any water lost to the rock matrix will remain trapped, thereby lowering the relative permeability to gas. In reservoirs with high initial water saturations, small variations in gas saturation can have dramatic repercussions on fractional flow, and therefore on well productivity.
3. Reservoir pressure: Damage around the fracture face induced by the loss of water-based fracturing fluids can be removed during flowback if the drawdown pressure exceeds the capillary forces holding the liquid in place. When the reservoir pressure is too low to create a drawdown pressure larger than the capillary forces, energized fluids are recommended.
4. Water sensitivity of the formation: In some rock formations, clay swelling, fines migration, and chemical reactions with the fracturing fluid can significantly reduce the rock permeability. Non-aqueous fluids are thus preferred: oil-base muds, LPG, CO_2, etc.
5. Proppant embedment: Many shales soften (reduction in the Young's modulus) when they are brought into contact with water-based fluids. This softening leads to additional proppant embedment and can lead to a significant loss in propped fracture conductivity. When this is determined to be the case (based on shale compatibility laboratory tests), non-aqueous fluids should be strongly considered, as they can prevent or at least minimize this effect.

Fluid Selection: Fracture Productivity, Cost, Availability, and Safety Hazards

The dimensionless fracture productivity is the most critical output because it is directly proportional to the initial well production for a given drawdown pressure. Using estimates of the production rate decline (following a hyperbolic, exponential, etc., model), one can obtain the incremental hydrocarbon production between two treatments solely by knowing the initial production. This is shown in **Fig. 13** for two arbitrary fracturing treatments having productivity indices of J_1 and J_2, respectively. In Fig. 13, q_a is the abandonment rate below which production is not economically viable anymore. The amount of incremental hydrocarbon is the area delimited by the two decline curves, which is indicated by the grey color in Fig. 13.

However, fluid selection is not limited to identifying the fluid that will generate the most revenues. Initial cost, availability, and safety hazards also come into the picture. In fact, much of the cost savings will depend on the availability of

the fluid and the structure of the pumping contractor's bid package. For example, the use of large quantities of CO_2 requires the deployment of many trucks, pressurized storage units, and additional pumping equipment. Safety hazards also hinder the use of some fluids (e.g., LPG which is very flammable and volatile). An extensive evaluation is then required to identify the risks and to define the steps minimizing those risks.

With this in mind, **Table 5** was constructed to clearly show the advantages and drawbacks of the most common energized fluids. Table 5 also lists the main factors that should be considered in fracturing fluid selection. In Table 5, a sign "✓" indicates that the fluid shows satisfactory performance; a "✗"indicates that the fluid performs poorly; and a "**?**" indicates that the impact of the fluid is unknown *a priori* and is strongly site-specific.

Conclusions

1. As with any design technique, there are many benefits and disadvantages to consider when selecting a fracturing fluid. A modeling approach is thus useful for fluid solution. It constitutes a cost-effective solution which complements costly field trials.
2. The combination of the compositional 3-D model introduced by Ribeiro and Sharma (2012b) and the PI model presented by Friehauf, Suri, and Sharma (2010) forms a design tool particularly suitable for designing and optimizing energized fracture treatments.
3. Energized fluids can usually produce hydrocarbon at higher productivities. These fluids (1) limit or eliminate the amount of liquid placed in the rock matrix (thereby minimizing liquid blocking), (2) improve the fluid recovery (due to the presence of free gas and soluble gas coming out of solution), and (3) minimize the contact between water and water-sensitive clays and fines.
4. Several reservoir parameters are critical for fluid selection: (1) relative permeability curves, (2) initial gas saturation, (3) reservoir pressure, (4) changes to the mechanical properties of the shale when contacted with the fracturing fluid and (5) the formation's sensitivity to water (clay swelling and fines migration). These factors control well productivity and, therefore, fluid selection.
5. Fluid selection also includes cost, availability, and safety considerations as outlined in Table 5.

Acknowledgements

The authors would like to acknowledge the support provided by RPSEA, the Department of Energy, and the companies sponsoring the JIP on *Hydraulic Fracturing and Sand Control* at the University of Texas at Austin (Air Liquide, Air Products, Anadarko, Apache, Baker Hughes, BHP Billiton, BP, Chevron, ConocoPhillips, ExxonMobil, Ferus, Halliburton, Hess Corporation, Linde Group, PEMEX, Pioneer Natural Resources, Praxair Inc., Saudi Aramco, Schlumberger, Shell, Southwestern Energy, Statoil, Weatherford, and YPF).

Nomenclature

E = Young's modulus, psi
F_{cd} = Dimensionless fracture conductivity
J = Productivity index
J_o = Productivity index of a un-fractured, undamaged reservoir in a circular drainage area
k = Reservoir permeability, mD
k_d = Invaded zone permeability, mD
$k_{rg,0}$ = Endpoint relative permeability of gas
L_f = Propped fracture length, ft
L_{re} = Outer drainage boundary radius, ft
n_g = Gas relative permeability exponent
q_a = Abandonment production rate, mcf/day
q_1, q_2 = Hydrocarbon production rate, mcf/day
$q_{1,i}$, $q_{2,i}$ = Initial hydrocarbon production rate, mcf/day
r_w = Wellbore radius, in
S_{wr} = Residual liquid phase saturation
S_{gr} = Residual gas phase saturation
ΔP = Drawdown pressure, psi
ν = Poisson's ratio

References

Burke, L.H., Nevison, G.W., and Peters W.E. 2011. Improved Unconventional Gas Recovery With Energized Fracturing Fluids: Montney Example. Paper SPE 149344 presented at the SPE Eastern Regional Meeting, Colombus, Ohio, 17–19 August 2011.

Economides, M.J. and Nolte, K.G. 2000. *Reservoir Stimulation*. John Wiley & Sons, LTD.

Friehauf, K.E. 2009. Simulation and Design of Energized Hydraulic Fractures. PhD Dissertation, The University of Texas at Austin, Austin, Texas (August 2009).

Friehauf, K.E., Suri, A., and Sharma, M.M. 2010. A Simple and Accurate Model for Well Productivity for Hydraulically Fractured Wells. *SPE Prod & Oper*, **25** (4): 453-460. SPE 119264-PA.

Gupta, S. 2011. Unconventional Fracturing Fluids: What, Where and Why. Technical Workshops for the Hydraulic Fracturing Study, US EPA, presented at Arlington, VA (February 2011).

Harris, P. 1985. Dynamic Fluid-Loss Characteristics of Nitrogen Foam Fracturing Fluids. *J Pet Technol* **37** (11): 1847-1852. SPE 11065-PA.

Harris, P. 1987. Dynamic Fluid-Loss Characteristics of CO_2-Foam Fracturing Fluids. *SPE Prod Eng* **2** (2): 89-94. SPE 13180-PA.

Harris, P., Klebenow, D.E., and Kundert, P. D. 1991. Constant-Internal-Phase Design Improves Stimulation Results. *SPE Prod Eng* **6** (1): 15-19. SPE 17532-PA.

Khade, K. and Shah, S. 2004. New Rheological Correlations for Guar Foam Fluids. *SPE Prod & Fac*, **19** (2): 77-85. SPE 88032-PA.

King, G.E. 1985. Foam and Nitrified Fluid Treatments-Stimulation Techniques and More. Paper SPE 14477 based on a speech presented as a Distinguished Lecture during the 1985-1986 season.

Mahadevan, J. and Sharma, M.M. 2005. Factors Affecting Cleanup of Water Blocks: A Laboratory Investigation. *SPE J.*,**10** (3): 238-246. SPE 103229-PA.

Mazza, R. 2001. Liquid-Free CO2/Sand Stimulations: An Overlooked Technology – Production Update. Paper SPE 72383 presented at the SPE Eastern Regional Meeting, Canton, Ohio, 17-19 October.

Parekh, B. and Sharma, M.M. 2004. Cleanup of Water Blocks in Depleted Low-Permeability Reservoirs. Paper SPE 89837 presented at the SPE Annual Technical Conference and Exhibition, Houston, Texas, 26–29 September 2004.

Reidenbach, V.G., Harris, P.C., Lee, Y.N, and Lord, D.L. 1986. Rheological Study of Foam Fracturing Fluids using Nitrogen and Carbon Dioxide. *SPE Prod Eng*, January, **1** (1): 31-41. SPE 12026-PA.

Ribeiro, L.H. 2013. Design of Energized Hydraulic Fractures. PhD Dissertation, The University of Texas at Austin, Austin, Texas.

Ribeiro, L.H. and Sharma, M.M.. 2012a. Multi-Phase Fluid-Loss Properties and Return Permeability of Energized Fracturing Fluids. *SPE Prod & Oper*, **27** (3): 265-277. SPE 139622-PA.

Ribeiro, L.H. and Sharma, M.M.. 2012b. A New Three-Dimensional Compositional Model for Hydraulic Fracturing with Energized Fluids. Paper SPE 159812 presented at the SPE Annual Technical Conference and Exhibition, San Antonio, Texas, 8–10 October 2012.

Tudor, E.H., Nevison, G.W., Allen, S., Pike, B. 2009. 100% Gelled LPG Fracturing Process: An Alternative to Conventional Water-Based Fracturing Techniques. Paper SPE 124495 presented at the SPE Eastern Regional Meeting, Charleston, West Virginia, 23-25 September 2009.

Valko, P. and Economides, M.J., 1997. Foam-Proppant Transport. *SPE Prod & Fac*, **12** (4): 244-249. SPE 27897-PA.

Vincent, M.C., 2002. Proving It - A Review of 80 Published Field Studies Demonstrating the Importance of Increased Fracture Conductivity. Paper SPE 77675 presented at the Annual Technical Conference and Exhibition, San Antonio, Texas , 29 September-2 October 2002.

Table 1—Basic reservoir properties (base-case scenario).

Reservoir Parameter	Value
Drainage Area (acre)	70
Wellbore Diameter (in)	3.875
Reservoir Temperature (°F)	180
Pay Zone Height (ft)	100
Permeability (mD)	0.01
Porosity (%)	13
Capillary Pressure (psi)	435
Residual Water Saturation	0.3
Residual Gas saturation	0.25
End-Point Permeability	0.6
End-Point Exponent	2.5

Table 2—Pumping schedule for all the fluid formulations.

Pumping Schedule	Stage 1	Stage 2	Stage 3
Duration (min)	15	10	25
Proppant loading (lbm/gal)	0	3	6
Rate (BPM)	25	20	20

Table 3—Fluid properties (evaluated at 110°F and 5000 psi and for the foam quality of interest)

Fluid Property	Slick Water	Linear Gel	CO_2	LPG	CO_2-foam 0.3	CO_2-foam 0.7	N_2-foam 0.7
Polymer (lbm/Mgal)	0	30	30	30	30	30	30
Density (lbm/ft^3)	62.4	62.4	52	33	59	55	31
Flow behavior index	1	0.508	0.8	0.8	0.508	0.508	0.508
Flow consistency index (lbf-s^n/ft^2) x10^3	0.018	7.3	0.50	0.26	7.3	30.2	30.2
Viscosity at 100s^{-1} (cp)	0.86	36	9.5	4.9	36	150	150
Leak-off coefficient (ft/√min) x10^3	2	0.5	0.5	0.5	0.28 / 0.04	0.15 / 0.08	0.15 / 0.08

Table 4—Fracture productivity (dimensionless form).

Quantity	Slick Water	Linear Gel	CO_2	LPG	CO2-foam 0.3	CO2-foam 0.7	N2-foam 0.7
L_f/L_{re}	0.3	0.16	0.22	0.20	0.21	0.26	0.24
F_{cd}	0.5	1.6	1.8	1.4	2.1	3.5	3.4
k_d/k	0.001	0.005	0.5	0.5	0.05	0.48	0.5
J/J_0	1.9	2.8	4.0	3.75	3.4	4.35	4.1

Table 5—Desired fracturing fluid properties.

Parameter	Slick Water	Linear Gel	Pure CO2	Pure N2	Foams	LPG
Fracture Creation	✓	✓	✓	✓	✓	✓
Wellbore Hydraulics	✓	✓	✓	×	?	✓
Proppant Transport	×	✓	?	×	✓	✓
Proppant Conductivity	×	×	✓	✓	✓	✓
Fluid Recovery	×	×	✓	✓	✓	✓
Reservoir Compatibility	?	?	✓	✓	✓	✓
Safety Hazards	✓	✓	?	?	?	×
Fluid Availability	?	?	?	?	?	?
Cost	✓	✓	?	?	?	?

A sign "✓" indicates that the fluid shows satisfactory performance; a "×"indicates that the fluid performs poorly; and a "?" indicates that the impact of the fluid is unknown a priori and is strongly site-specific.

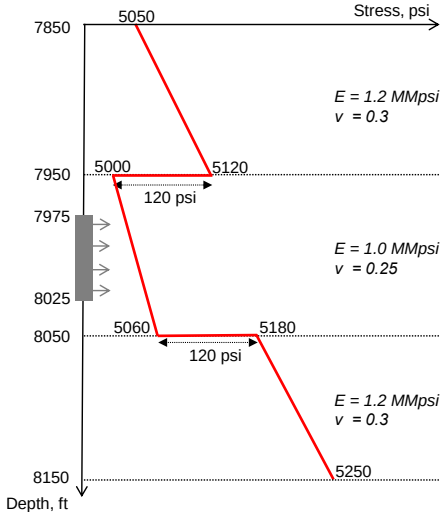

Figure 1—*In-situ* horizontal stress distribution, Young's modulus, and Poisson's ratio for the base-case scenario.

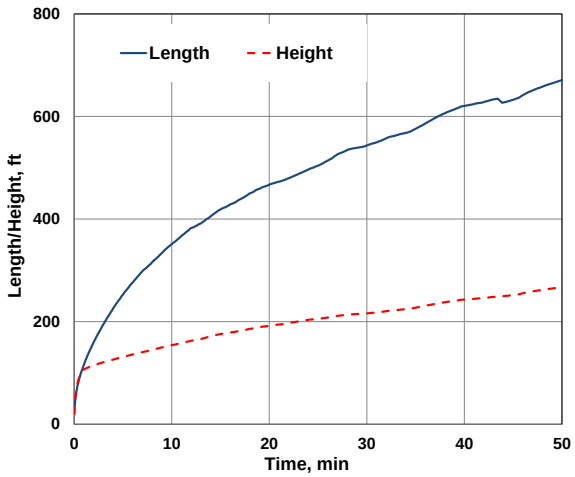

Figure 2—Fracture length and fracture height during pumping for 0.7-quality CO_2 foam.

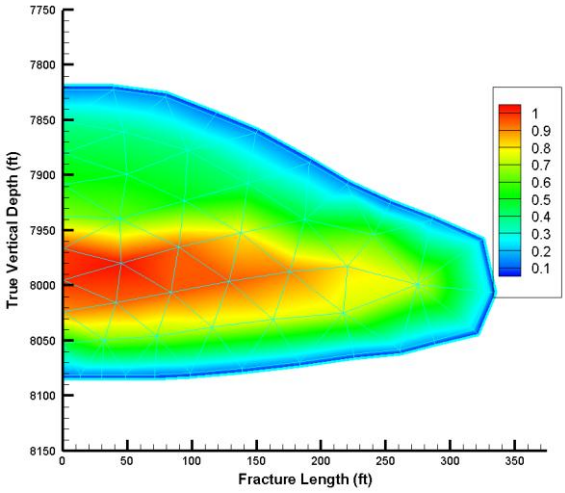

Figure 3—Fracture width (inches) for 0.7-quality CO_2 foam.

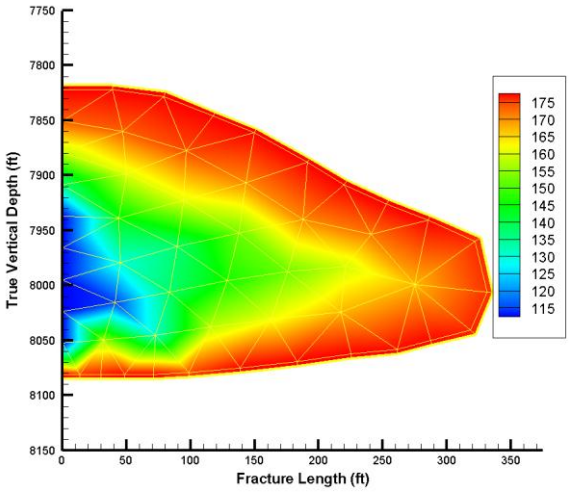

Figure 4—Fluid temperature (°F) for 0.7-quality CO_2 foam.

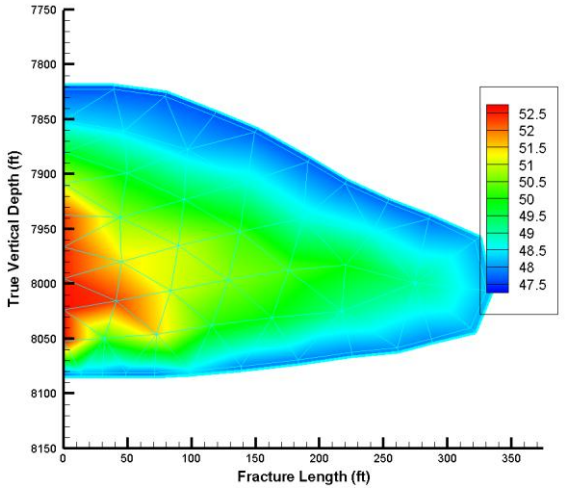

Figure 5—CO_2 gas phase density (lbm/ft^3) for 0.7-quality CO_2 foam.

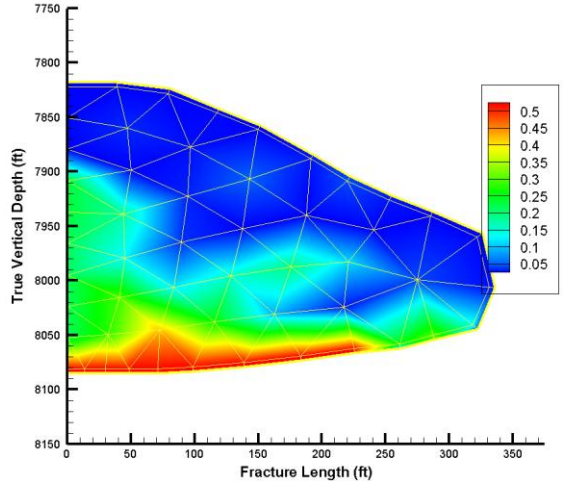

Figure 6—Volumetric proppant concentration for 0.7-quality CO_2 foam.

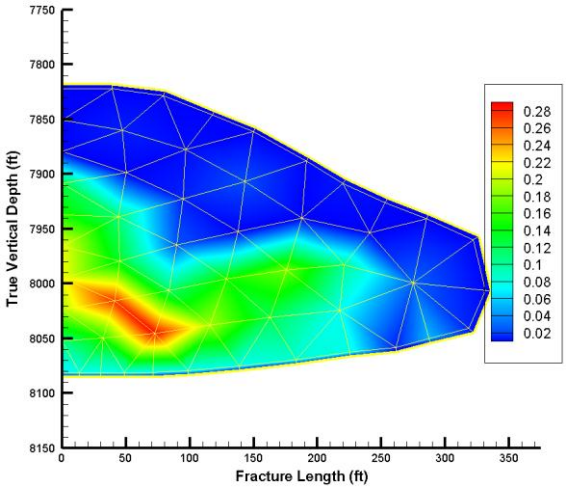

Figure 7—Propped fracture width (inches) for 0.7-quality CO_2 foam.

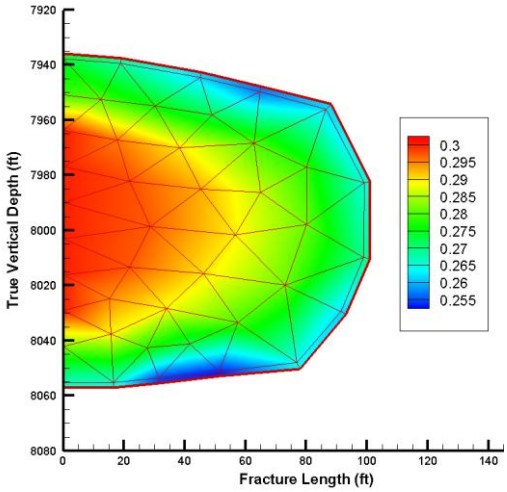

Figure 8—Water saturation for stable 0.7-quality CO_2 foam after 5 minutes of pumping.

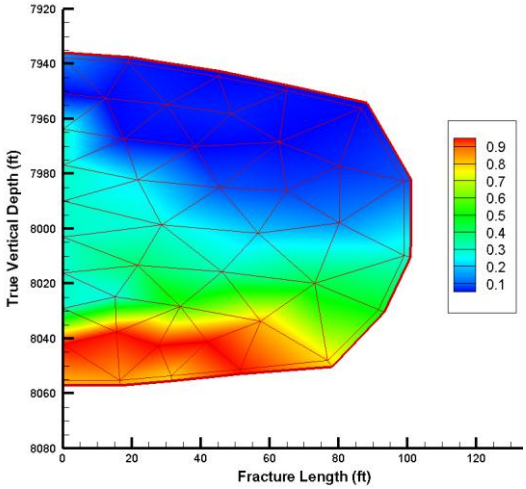

Figure 9—Water saturation for unstable 0.7-quality CO_2 foam after 5 minutes of pumping.

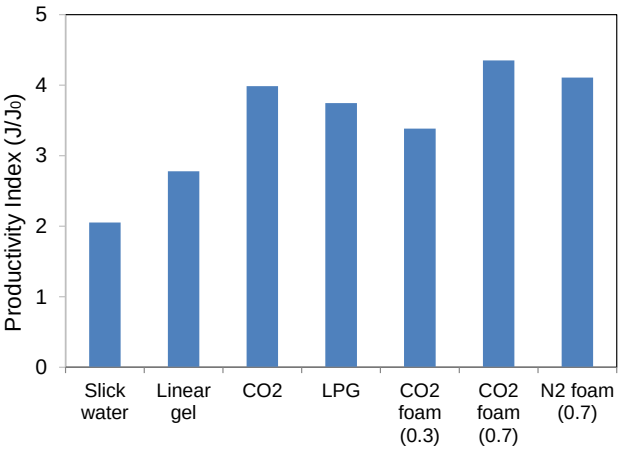

Figure 10—Comparison of the productivity index (J/J_0) for the different fluid formulations. The energized fluids outperform slick water and linear gel in this particular example.

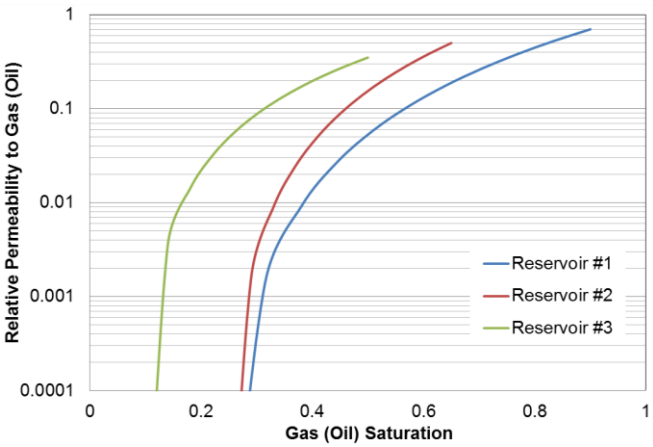

Figure 11—Typical relative permeability curves in three reservoirs, which are representative of (1) dry gas reservoir, (2) intermediate reservoir, and (3) strongly water-wet reservoir.

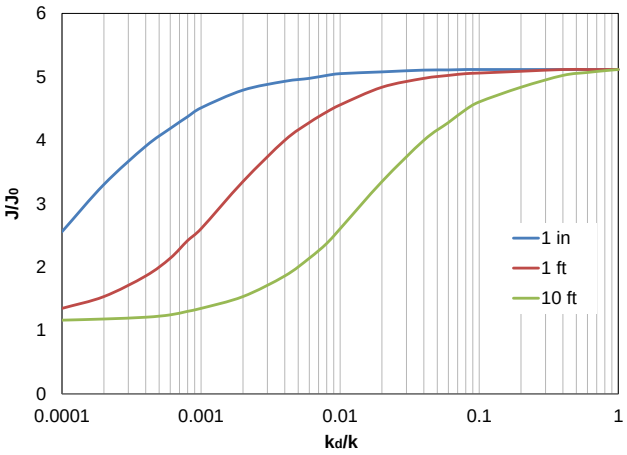

Figure 12—Impact of the depth of penetration and of the effective permeability in the invaded zone on the fracture productivity index (J/J_0).

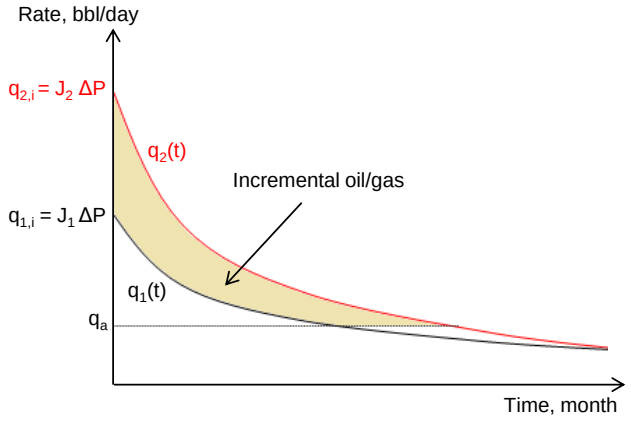

Figure 13—Incremental hydrocarbon production as a function of initial fracture productivity for two arbitrary treatments with productivity indices J_1 and J_2.